Defence Science Journal, Vol. 68, No. 4, July 2018, pp. 347-355, DOI : 10.14429/dsj.68.11349

Failure Behaviour of Concrete, Subjected to High Dynamic Loading of New Spiral Projectile

Jun Wu, Jianguo Ning, and Tianbao Ma*

State Key Laboratory of Explosion Science and Technology, Beijing Institute of Technology, Beijing - 100 081, China
**E-mail: madabal@bit.edu.cn*

ABSTRACT

A new spiral warhead structure which makes concrete failure by self-rotation is proposed. Concrete dynamic response when subjected to the oval and new proposed spiral projectile with vertical and oblique-angle (from 60° to 70°) impacts of different velocities is studied numerically. The data relating projectile residual velocity with different rotation angles and groove depths is plotted and interpreted when concrete target subjected to the impact loading ranging from 700 m/s ~ 1000 m/s. The rotational angular velocity *vs* time curves for different working condition are also obtained.

Keywords: Dynamic response; Concrete; Spiral warhead; Penetration

1. INTRODUCTION

Concrete has been widely used in the field of civil and military engineering[1-3]. Damage effects analysis of concrete or reinforced concrete buildings under impact loading is an important problem concerned by the area of collision accident analysis, shock-resistant design and military weapon design.

A number of studies are performed experimentally, analytically and numerically to describe various penetration problems. Sandia National Laboratory and Waterways Experiment Station conducted systematic investigations of penetration mechanism, projectile material, the law of trajectory, dynamic structural response, different target media penetration attributes and so on. Young formula[4] which based on large amount of experimental data was used to estimate the vertical penetration depth of the projectile, and it was expressed as a function of projectile geometry, initial velocity, projectile mass and target material. Ben-Dor[5] suggested an approach that allows deriving penetration equations using semi-empirical analytical dependence between the impact velocity and the depth of penetration. Bernard[6-7] proposed an empirical formula for projectile penetrating into rock and concrete which contains a projectile head shape factor Caliber-Radius-Head, the density and uniaxial compressive strength of the target material, and the target rock quality index RQD (rock quality Designator) was brought in. Forrestal[8-9], Frew[10] and Hanchak[11], *et al.* conducted a lot of penetration experiments of projectile into concrete targets. Goldsmith and Backman[12-13] summarised analytical, numerical and experimental investigations of non-ideal projectile impact on targets, including oblique impact, yaw impacts and ricochet. Chen[14], *et al.* and Warren[15], *et al.* carried the experiments of oblique penetration. Li[16] summarised the empirical formulae which used to predict the penetration depth. He compared various nose shape factors and suggested a unique definition of the nose shape factor. Chen[17-18], proposed a general non-dimensional formula based on the dynamic cavity-expansion model to predict penetration depth subjected to the impact of a non-deformable projectile. He[19], *et al.* analysed the penetration process considering mass loss. In the study of the constitutive model, dynamic constitutive models have been developed for describing various damage and failure behaviours of concrete during penetration process[20-22]. The efforts were also extended to improved and developed constitutive model[23-24] and validate these models by numerical simulations ways[25-27].

The structure of warhead is improved and the spiral projectile model is proposed. There was no prior research work on spiral warheads. In this investigation, various working conditions of the spiral projectile and the oval projectile vertical and oblique-angle penetrating concrete targets are compared. A parametric study is carried out to explore the influence of spiral projectile structural parameters on the penetrating effect. In addition, the numerical simulation verification of the test of oval projectile penetrating the reinforced concrete has been carried out, which shows the reasonable of the modelling method and the selection of the parameters in this paper.

2. THE MECHANISM OF SPIRAL PENETRATION

Factors that can affect the ability of the projectile penetration mainly divided into three categories: one is the kinematic factors, such as the projectile initial velocity, impact gesture and so on; the second is the structural factors, such as the aspect ratio of penetrator, bullet shape; third is material of projectile. The kinematic factors are decided and restricted by its launch platform. Restricted by the launch platform, the length-diameter ratio of projectile has a strong constraint. The

Received : 22 April 2017, Revised : 26 March 2018
Accepted : 20 April 2018, Online published : 25 June 2018

mechanical properties of the projectile material depend on the smelting technology, alloy ratio and so on. The head shape has a weak constraint and a larger space for improvement[28-29].

Most of the projectile adopted the ogive shape or structure that is the oval projectile. In this investigation, a spiral structural warhead is proposed. It will produce torque in the interaction between its own structure and the concrete target, and this lead the concrete material tension failure and shear failure. Because the concrete tensile strength and shear strength are far smaller than the compressive strength, the spiral structural warhead can save more kinetic energy and improve the projectile's penetration efficiency. The mechanism is as shown in Fig. 1.

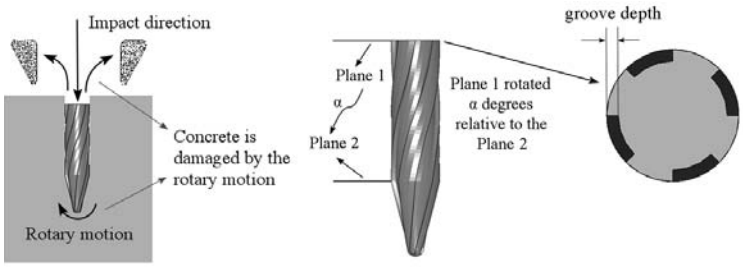

Figure 1. The working principle of spiral penetrating.

3. NUMERICAL SIMULATION CONTRAST OF SPIRAL WARHEAD AND OVAL WARHEAD PENETRATION

The vertical and oblique penetration of spiral projectile and oval projectile into concrete boards at different velocities are simulated using the finite element code LS-DYNA.

3.1 Finite Element Model

The projectile length is 52.4 mm and diameter is 12.16 mm. The oval projectile caliber-radius head ratio is 2.06. The spiral projectile groove depth is 1.08 mm. The mass of the oval warhead and the spiral warhead is 40.212 g and 33.402 g, respectively. The two projectiles geometry structures are as shown in Fig. 2. The concrete target board of the vertical penetration is a cylinder, and the board size is φ 300 mm × 200 mm. The oblique penetration concrete target is a rectangular block and the size is 400 mm × 200 mm × 200 mm. The thickness of concrete target ensures that the interaction between the projectile and concrete target last for a period of time. This ensures sufficient interaction between the projectile and target during the penetration process.

The projectile/target finite element model is meshed with eight-node solid elements, and all the elements are hexahedral grid. Because the structure of spiral projectile is asymmetric, it adopts full model modelling. The oval projectile adopts a quarter modelling for its symmetry. Non-reflective boundaries are used on the lateral faces to represent the semi-infinite target. The algorithm "eroding surface to surface" of LS-DYNA is used to define the contact between the target and the projectile.

3.2 Material Model of Concrete and Projectile

The concrete adopts the Johnson-Holmquist concrete constitutive model which wildly used to describe the dynamic behaviours of the concrete subjected to large strain at high

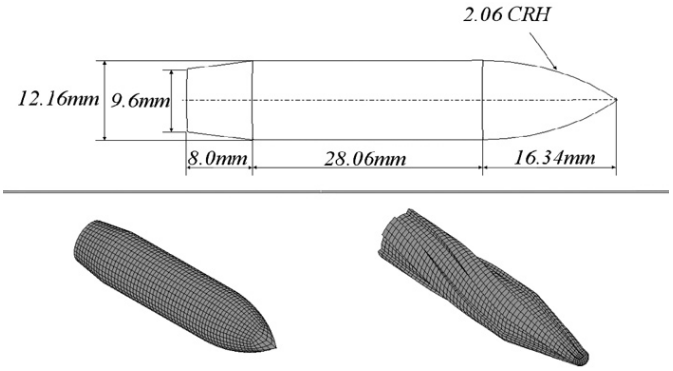

Figure 2. The geometry and finite element model of oval projectile and the spiral projectile.

pressure and high strain rates. The material parameter of the concrete[25], the concrete density is 2.44 g/cm^3, the compressive strength is 48 MPa and the shear modulus is 14.86 GPa. The algorithm 'Mat Add Erosion' of LS-DYNA is brought in, and this combined method can simulate the open pit and the crack propagation situation of the concrete better. The indicators of concrete failure select the negative pressure and maximum plastic strain in this study. By verifying existing penetration test repeatedly, the threshold of maximum negative pressure and maximum plastic strain are set as 4 Mpa and 0.7 Mpa, respectively. Once the criterion reaches a preset value, the element will be removed. The energy of deleted element is transmitted to other adjacent units in the calculation.

The plastic/kinematic material model[30] is used for the projectile. This model is suited to simulate isotropic and kinematic hardening of plasticity with the condition of including rate effects. Parameters of the projectile[25], the projectile density is 8.0 g/cm^3, the Young's modulus is 207 GPa, the Poisson's ratio is 0.3 and the Yield stress is 1724 MPa.

3.3 Simulation Results and Analysis

Conditions of the spiral and oval projectiles penetrating concrete target with the same impacting speeds ranging from 600 m/s to 1000 m/s are simulated.

The residual velocities of the two kind projectiles at different initial velocity were as given in Table 1. The spiral projectile residual velocity is higher by 15.1 % - 28.2 % than that of the oval projectile. The spiral projectile residual kinetic energy is by higher by 18.78 % - 28.72 % than that of the oval projectile. It should be noted that the spiral projectile is not rotating about its axis before it hit the target. When the projectiles pass through the target, the spiral projectile has translational velocity and angular velocity, and the oval projectile only has translational velocity. The measured as well as the calculated percentage of residual kinetic energy here includes the translational velocity, but don't include the angular velocity. The spiral projectile demonstrates better penetrating effectiveness.

The spiral projectile angular velocity and its maximum value demonstrate an increasing trend with the increase of impacting velocity, as shown in Fig. 3. A maximum rotational angular velocity 0.0134 rad/μs can be produced

Table 1. Comparison of residual velocity and residual kinetic energy

V_0 (m/s)	Kind of projectile	Vr (m/s)	Percentage of residual kinetic energy (%)
600	Oval projectile	383.4	40.89
	Spiral projectile	484.95	65.68
700	Oval projectile	466.32	44.49
	Spiral projectile	597.86	73.21
800	Oval projectile	563.2	49.68
	Spiral projectile	689.31	74.5
900	Oval projectile	640.23	50.8
	Spiral projectile	789.32	77.14
1000	Oval projectile	756.47	57.29
	Spiral projectile	870.74	76.07

by the spiral warhead at 1000 m/s initial impacting velocity. The displacement vectors of spiral projectile in the XY-plane (perpendicular to the impacting velocity) are as shown in Fig. 3. It shows that the projectile can achieve rotational motion in the high-speed penetration process.

The rotation angle and the groove depth are the main structural parameters of the spiral projectile. In order to explore the influence of spiral projectile structural parameters on the penetrating effect, the parametric study is carried out.

In addition to the α value of 90° simulated in the previous section, α value of 60°, 75°, 105° and 120° are also simulated. The residual velocity corresponding to each α value for the different initial velocities ranging from 700 m/s-1000 m/s are

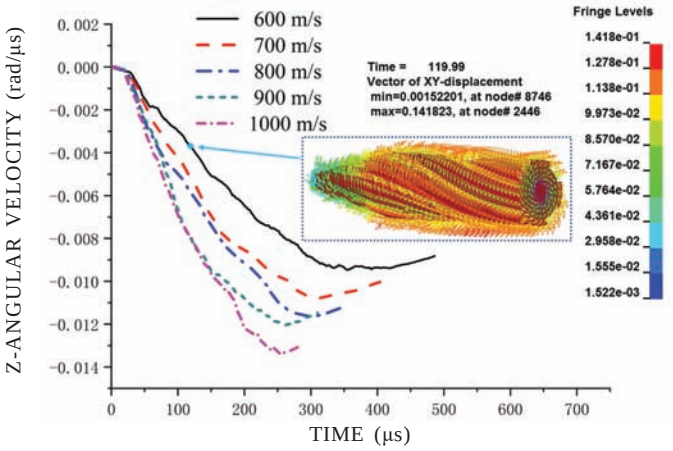

Figure 3. Angular velocity vs tine curve of different initial velocities.

as shown in Fig. 4. With the increase of the rotation angle, the residual velocity of projectile first increases and then decreases. When the rotation angle of the spiral projectile is around 86° ~ 91°, the optimal residual velocity will be obtained.

Figure 5 gives the rotational angular velocity *vs* time curves for different initial velocities and rotation angles. The rotational angular velocity value shows an increasing trend with the increase of α. It shows that for the velocity 700 m/s and α = 120°, the spiral warhead maximum angular velocity can reach 0.0117 rad/μs. With the initial velocity 800 m/s, 900 m/s and 1000 m/s, the maximum angular values are up to 0.0152 rad/μs, 0.0160 rad/μs and 0.0176 rad/μs, respectively.

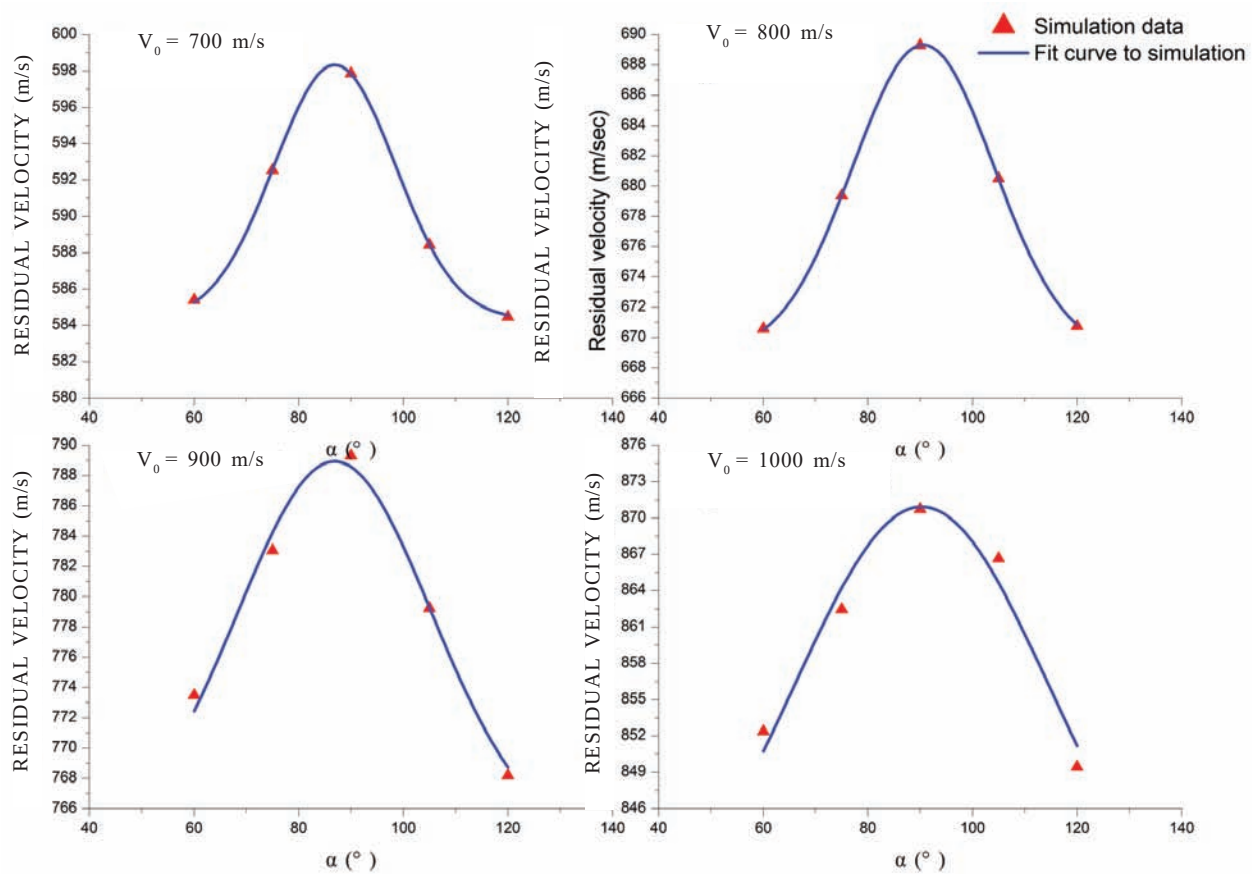

Figure 4. Comparison of residual velocity with different initial velocities.

As above investigation, the groove depth is 1.08 mm and rotation angle α = 90°. Next, conditions of rotation angle α = 90° and groove depth value of 0.5 mm, 0.75 mm, 1.25 mm and 1.5 mm are also simulated. Figure 6 gives the residual velocity corresponding to different groove depth with the initial velocities ranging from 700 m/s - 1000 m/s. When the initial velocity ranging from 700 m/s - 900 m/s, the projectile residual velocity first increases and then decreases with the increase of the groove depth. When the initial velocity arrive 1000 m/s, the projectile residual velocity increases with the growth of groove depth within a certain range. From the overall situation of four curves, it can be inferred that the change of optimal projectile residual velocity would be a dynamic change process. When the initial velocity gradually increases, the residual velocity rises with the increase of the groove depth.

Figure 7 gives the rotational angular velocity *vs* time curves for different initial velocities and groove depth when the rotation angle is 90°. When the initial velocity is constant, the rotational angular velocity and its maximum value show an increasing trend with the increase of the groove depth.

In the previous study, the projectile penetrates the target vertically. Generally, the oblique-angle penetration occurs more frequently than the normal penetration does, even ricochet occurs. The oblique angle θ ($0 < \theta < 90°$) is defined as the acute angle between the velocity of the projectile and the outward normal of the impact surface of the target. As the ricochet phenomenon seriously affects the penetration depth of the projectile and the rule of the overload, oblique-angle penetration of two type projectiles are carried out. The projectile impacts the concrete target in different oblique angles ranging from 60° to 70°, and the initial velocities ranging from 700 m/s to 1000 m/s.

When the oblique angle is 60° and velocity is 700 m/s, ricochet occurs. Figure 8 shows concrete's damage pattern at different times and the ballistic trajectory of the spiral projectile. *L* is the length of the ballistic trajectory and *P* is the maximum penetration depth. *T* is the total time of the interaction between the projectile and the target. θ is the oblique angle. Other conditions presented in Table 2 show the two types of projectiles ballistic parameters under different working conditions.

Table 2. Characteristics of the oblique penetrating trajectory

V_0 (m/s)	Type of projectile	θ (°)	*Vr* (m/s)	*T* (us)	*P* (cm)	*L* (cm)	State
700	Oval projectile	60°	174.29	902	7.05	29.12	Ricochet
	Spiral projectile		296.02	800	7.99	29.38	Ricochet
800	Oval projectile	63°	240.53	739.99	7.12	28.83	Ricochet
	Spiral projectile		379.97	615	7.33	27.56	Ricochet
900	Oval projectile	66°	259.73	664.99	7.43	29.53	Ricochet
	Spiral projectile		451.18	515	7.23	26.73	Ricochet
1000	Oval projectile	70°	418.67	469.99	6.01	27.20	Ricochet
	Spiral projectile		499.18	455	5.31	30.47	Ricochet

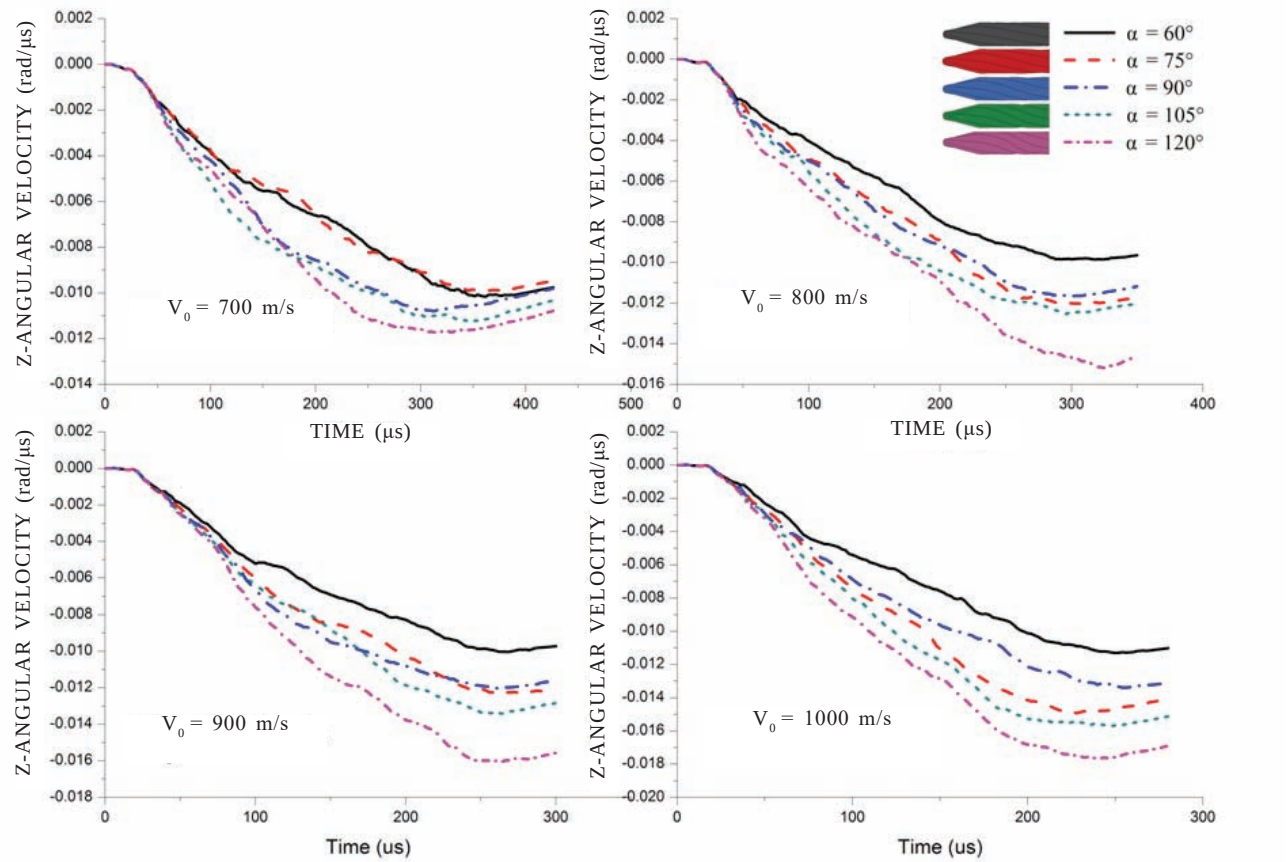

Figure 5. Angular velocity *vs* time curve of different α value with various initial velocities.

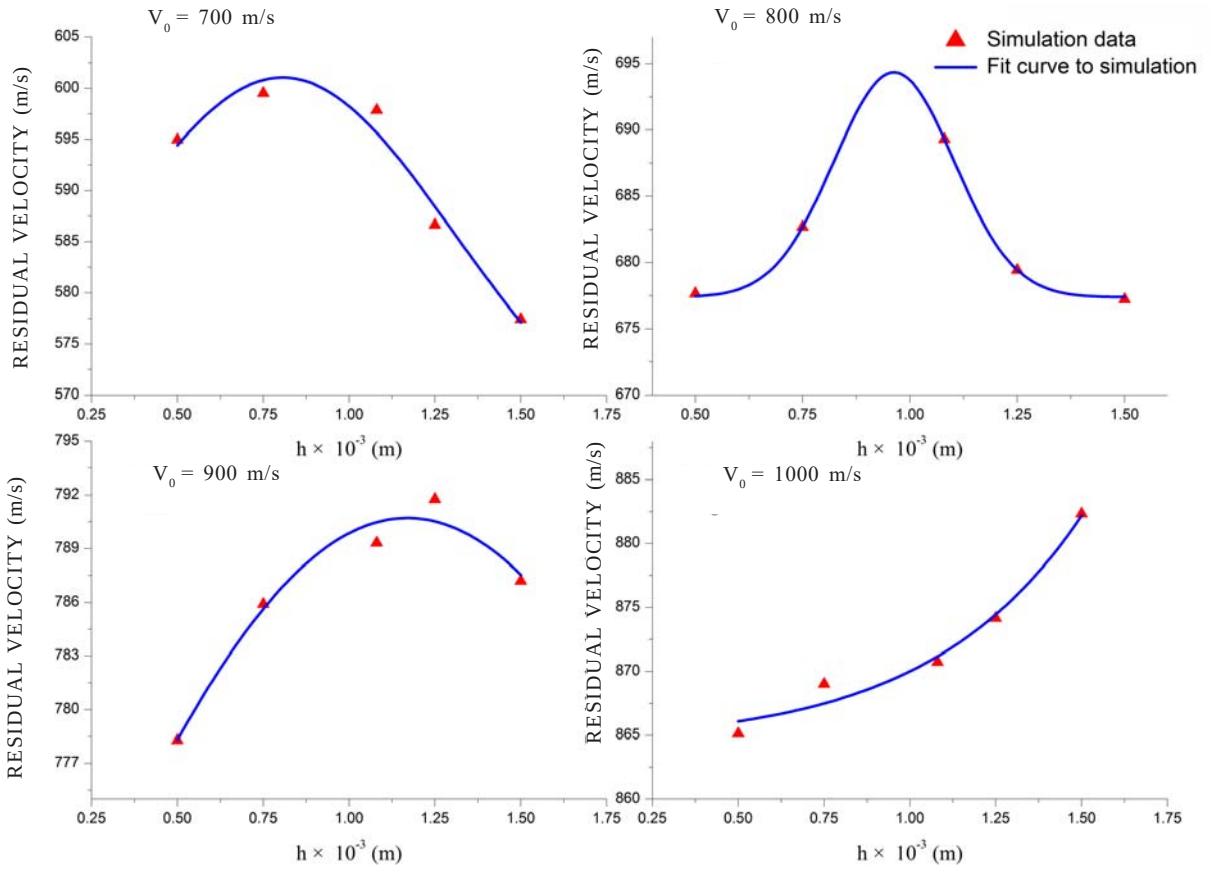

Figure 6. Comparison of residual velocity with different initial velocities.

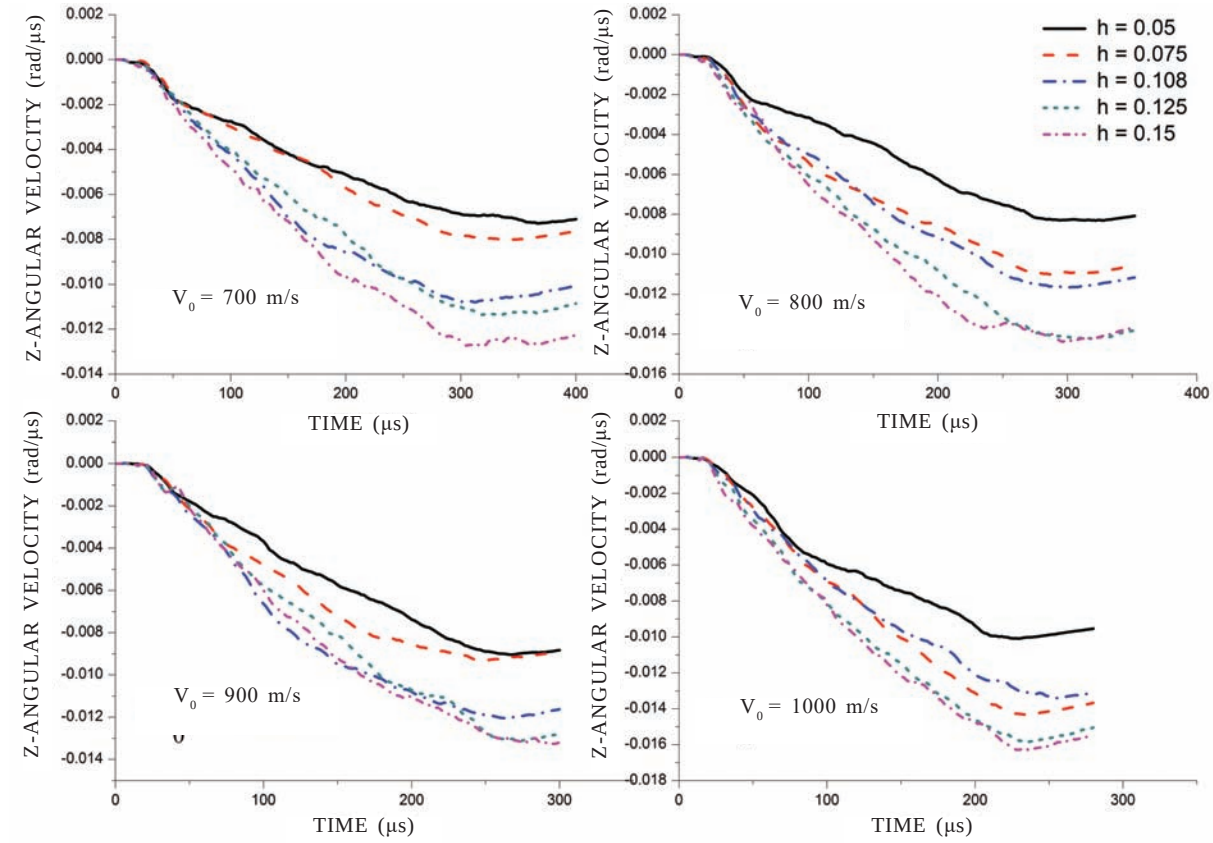

Figure 7. Angular velocity curve of different groove depth value with various initial velocities.

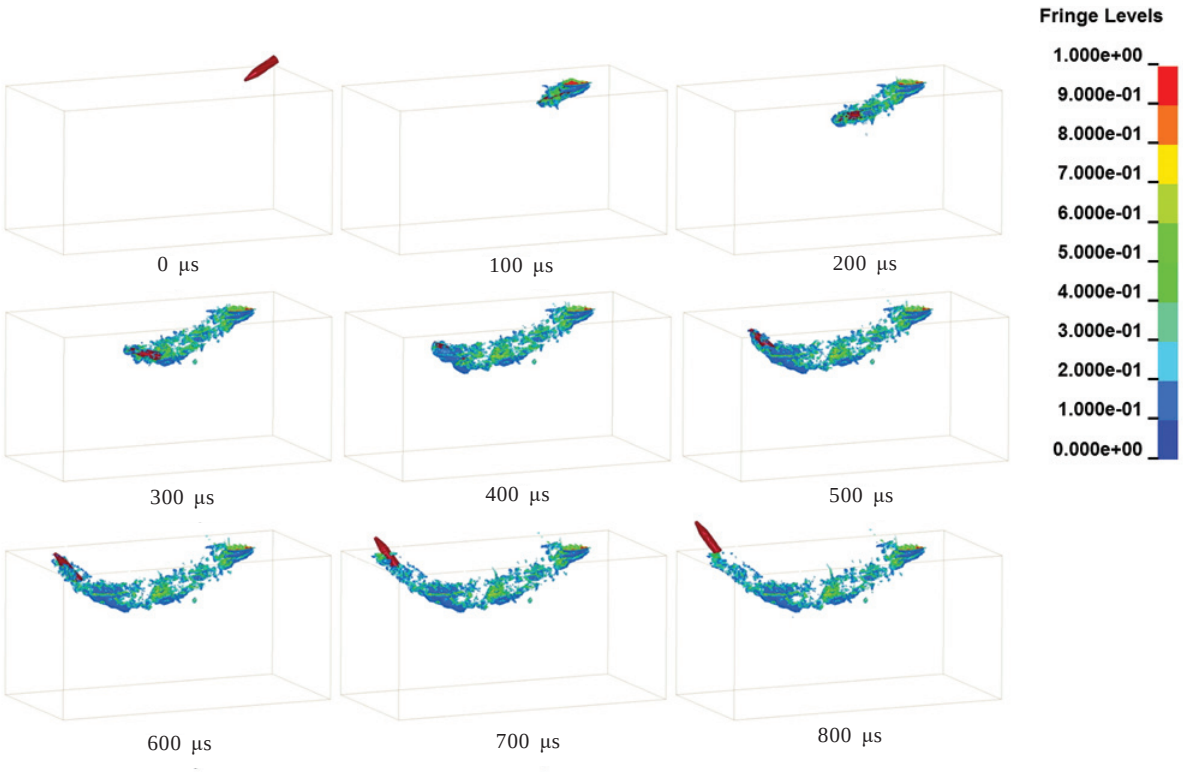

Figure 8. Concrete's damage pattern at different times under the spiral projectile with a speed of 700 m/s and oblique angle 60°.

The existence of the oblique angle makes the reflection stretching wave asymmetric, the projectile and the concrete subjected to imbalance force. The damage accumulation caused by reflected tensile wave make the concrete above the ballistic trajectory form cracks. Chunks of concrete break off and part of the concrete avalanched from the target.

It can be seen from the data in Table 2, the interaction time between spiral projectile and concrete board is shorter than the oval projectile, and the residual velocity of spiral projectile is higher than the oval projectile. When the initial velocity is ranging from 700 m/s - 800 m/s, the ballistic penetration depth of spiral projectile is higher than the oval projectile, and their ballistic lengths are similar. When the initial velocity is ranging from 900 m/s - 1000 m/s, the ballistic penetration depth of spiral projectile is smaller than the oval projectile. Numerical results show that the well penetration effect of spiral projectile depends on the stable contact between the projectile and the concrete target. In the premise of stable contact between the projectile and the target plate, the longer the interaction time, the spiral projectile penetrating performance more obvious.

4. NUMERICAL CONFIRMATORY OF THE PROJECTILE PENETRATING REINFORCED CONCRETE TARGET

In order to verify the reliability of numerical simulation, Hanchak. SJ´s experiment is simulated. Hanchak[11], *et al.* carried out perforation experiments with ogival nose rods, 3.0 caliber radius head, 25.4 mm diameter, 143.7 mm length, 0.5 kg and 610 mm × 610 mm × 178 mm reinforced concrete slabs with 48 MPa and 140 MPa unconfined compressive strength. The concrete board reinforced with three levels of orthogonal rebar with mesh size 76.2 mm × 76.2 mm, and the diameter of rebar is 5.69 mm. The projectile impacts the reinforced concrete target with different initial velocities ranging from 300 m/s to 1100 m/s.

Only a quarter of the board is simulated because of symmetry. Both sides of the target plate boundary applied fixed support, and lateral faces of the target applied non-reflective boundaries. Contact between the target and the projectile adopted algorithm of "eroding surface to surface".

The dynamic response of rebar is described by the plastic/kinematic material model. The material parameters of the rebar[25] are as below: ρ = 7.5 g/cm^3, E = 210 GPa, Fs = 0.8, SIGY = 235 MPa, PR = 0.3. The parameters of the 48 MPa concrete and projectile are the same with Section 3.2.

In this part, all conditions about the reinforced concrete target impacted by the projectile with different speeds (in the experiment) are simulated.

Comparison of numerical simulation and experiment results (749 m/s initial velocity, reinforced concrete slabs with 48 MPa unconfined compressive strength) is shown in Fig. 9. Phenomenon of concrete cross-section near the surface is consistent with the experimental results. The stress pattern of the top and bottom steel mesh is shown as follows.

Residual velocity under different working condition obtained by numerical simulation is compared with the test results, as shown Fig. 10. Comparing results show that the material parameters and modelling methods reliable.

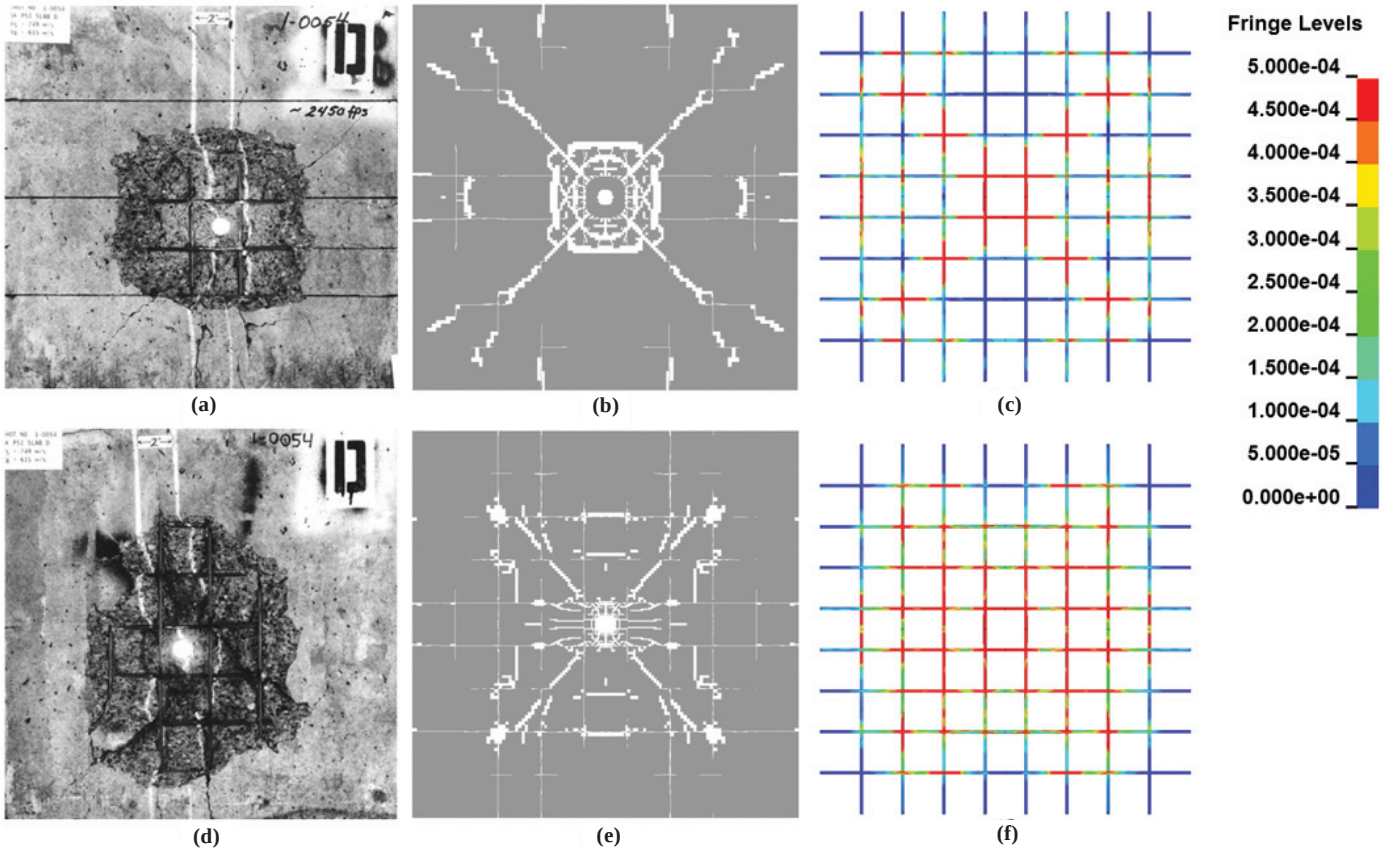

Figure 9. Comparison between post-test impact surface (a) and the front surface of numerical simulation (b); comparison between post-test rear surface (d) and the back surface of numerical simulation (e); stress pattern of the top (c) and bottom (f) steel mesh.

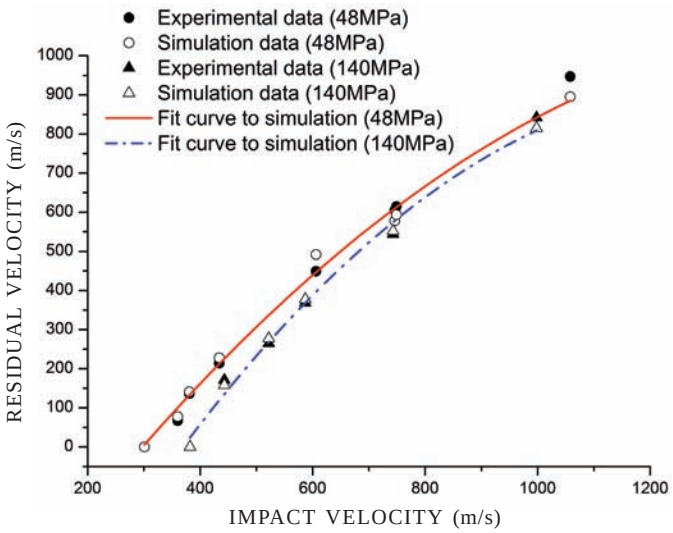

Figure 10. Comparison of experimental and numerical results.

5. CONCLUSIONS

With high initial velocity, the new spiral warhead can achieve rotary motion by the interaction with the concrete during the penetration process, and then torque produced by the rotary motion makes the concrete material failure.

The numerical results show that the residual velocity and kinetic energy residual proportion of spiral projectile were higher than those of oval projectile by 28.2 per cent and 28.7 per cent at most with the same working condition. The penetrating effects with different rotation angle and groove depth are compared and the rotational angular velocity-time curves with different rotation angle or different groove depth for different initial velocities are obtained.

The ballistic trajectories of spiral projectile and oval projectile with oblique penetration are compared by numerical simulation. The result indicates that in the premise of stable contact between the projectile and the concrete target, the longer the interaction time, the spiral projectile penetrating performance more obvious.

REFERENCES

1. Bruno, S.; & Valente, C. Comparative response analysis of conventional and innovative seismic protection strategies. *Earthquake Eng. Struct. Dyn.*, 2002, **31**, 1067-1092. doi: 10.1002/eqe.138.
2. Morales-Alonso, G.; Cendon, D.A. & Galvez, F.V. & Sanchez-Galvez. Influence of the softening curve in the fracture patterns of concrete slabs subjected to blast. *Engng. Fract. Mech.*, 2015, **140**, 1-16. doi: 10.1016/j.engfracmech.2015.03.035.
3. Zhan, T.B.; Wang, Z.H. & Ning, J.G. Failure behaviours of reinforced concrete beams subjected to high impact loading. *Eng. Fail. Anal.*, 2015, **56**, 233-243. doi: 10.1016/j.engfailanal.2015.02.006.

4. Young, C.W. Penetration Equations. SAND97-2426. Albuquerque, NM: Sandia National Laboratories., 1997.
5. Ben-Dor, G. & Dubinsky A. & Elperin T. Engineering approach to penetration modeling. *Engng. Fract. Mech*., 2008, **75**, 4279-4282. doi: 10.1016/j.engfracmech.2008.03.016.
6. Bernard, R.S. Development of a projectile penetration theory. Report 2: Deep penetration theory for homogeneous and layered targets. United States Waterways Experiment Station, Vicksburg, Miss; 1976.
7. Bernard, R.S. & Hanagud, S.V. Development of a projectile penetration theory. Report 1: Penetration theory for shallow to moderate depths. United States Waterways Experiment Station, Vicksburg, Miss; 1975.
8. Forrestal, M.J.; Frew, D.J.; Hickerson, J.P. & Rohwer, T.A. Penetration of concrete targets with deceleration-time measurements. *Int. J. Impact Eng*., 2003, **28**, 479-497. doi: 10.1016/S0734-743X(02)00108-2.
9. Forrestal, M.J.; Frew, D.J.; Hanchak, S.J. & Brar, N.S. Penetration of grout and concrete targets with ogive-nose steel projectiles. *Int. J. Impact Eng.*, 1996, **18**, 465-476. doi: 10.1016/0734-743X(95)00048-F.
10. Frew, D.J.; Forrestal, M.J. & Hanchak, S.J. Penetration experiments with limestone targets and ogive-nose steel projectiles. *J. Appl. Mech-T ASME*., 2000, **67**, 841-845. doi: 10.1115/1.1331283.
11. Hanchak, S.J.; Forrestal, M.J.; Young, E.R. & Ehrgott, J.Q. Perforation of concrete slabs with 48 MPa (7 ksi) and 140 MPa (20 ksi) unconfined compressive strengths. *Int. J. Impact Eng*., 1992, **12**(1), 1-7. doi: 10.1016/0734-743X(92)90282-X.
12. Goldsmith, W. Non-ideal projectile impact on targets. *Int. J. Impact Eng*., 1999, **22**, 95-395. doi: 10.1016/S0734-743X(98)00031-1.
13. Backman, M.E.; Goldsmith, W. Mechanics of penetration of projectiles into targets. *Int. J. Eng. Sci*., 1978, **16**, 1–99. doi: 10.1016/0020-7225(78)90002-2.
14. Chen, X.W.; Fan, S.C. & Li, Q.M, . Oblique and normal perforation of concrete targets by a rigid projectile. *Int. J. Impact Eng*., 2004, **30**, 617-637. doi: 10.1016/j.ijimpeng.2003.08.003.
15. Warren, T.L.; Hanchak, S.J. & Poormon, K.L. Penetration of limestone targets by ogive-nosed VAR 4340 steel projectiles at oblique angles: experiments and simulations. *Int. J. Impact Eng*., 2004, 30, 1307-1331. doi: 10.1016/j.ijimpeng.2003.09.047.
16. Q.M, Li.; Reid, S.R.; Wen, H.M. & Telford, A.R. Local impact effects of hard missiles on concrete targets. *Int. J. Impact Eng*., 2005, **32**, 224-284. doi: 10.1016/j.ijimpeng.2005.04.005.
17. Chen, X.W. & Li, Q.M. Deep penetration of truncated-olive-nose projectile into concrete target. *In* Proceeding of the 4th International Symposium on Impact Engineering, Kumamoto, Japan; 2001
18. Chen, X.W. & Li, Q.M. Deep penetration of a non-deformable projectile with different geometrical characteristics. *Int. J. Impact Eng*., 2002, **27**, 619-637. doi: 10.1016/S0734-743X(02)00005-2.
19. He, L.L. & Chen, X.W. Analyses of the penetration process considering mass loss. *Eur. J. Mech. A-Solid*., 2011, **30**, 145-157. doi: 10.1016/j.euromechsol.2010.10.004.
20. Taylor, LM.; E.P, Chen. & Kuszmaul, J.S. Microcrack-include damage accumulation in brittle rock under dynamic loading. *Comput. Methods Appl. Mech. Eng*., 1986, **55**(3), 301-320. doi: 10.1016/0045-7825(86)90057-5.
21. Holmquist, T.J.; Iohnson, G.R. & Cook, W.H. A computational constitutive model for concrete subjected to large strains, high strain rates and high pressure. *In* Proceeding of the fourteenth international symposium on ballistics, Quebec, Canada; 1993, 591-600.
22. Riedel, W.; Thoma, K.; Hiermaier, S. & Schmolinske, E. Penetration of reinforced concrete by BETA-B-500 numerical analysis using a new macroscopic concrete model for hydrocodes. *In* Proceedings of the ninth international symposiumon interaction of the effects of munitions with structures, Berlin, Germany; 1999, 315–322.
23. Polanco-Loria, M.; Hopperstad, O.S.; Borvik, T. & Berstad, T. Numerical predictions of ballistic limits for concrete slabs using a modified version of the HJC concrete model. *Int. J. Impact Eng*., 2008, **35**, 290-303. doi: 10.1016/j.ijimpeng.2007.03.001.
24. Tu, Z. & Lu, Y. Modifications of RHT material model for improved numerical simulation of dynamic response of concrete. *Int. J. Impact Eng*., 2010, **37**, 1072-1082. doi: 10.1016/j.ijimpeng.2010.04.004.
25. Liu, Y.; Huang, F.L. & Ma, Aie. Numerical simulations of oblique penetration into reinforced concrete targets. *Comput Math Appl*., 2011, **61**, 2168-2171. doi: 10.1016/j.camwa.2010.09.006.
26. Liu, Y.; Ma, Aie & Huang, F.L. Numerical simulations of oblique-angle penetration by deformable projectiles into concrete targets. *Int. J. Impact Eng*., 2009, **36**, 438-446. doi: 10.1016/j.ijimpeng.2008.03.006
27. Islam, M.J.; Swaddiwudhipong, S. & Liu, Z.S. Penetration of concrete targets using a modified Holmquist-Johnson-Cook material model. *Int. J. Comp. Meth*., 2012, **9**, 4. doi: 10.1142/S0219876212500569.
28. Ben-Dor, G.; Dubinsky A. & Elperin T. Numerical solution for shape optimization of an impactor penetrating into a semi-infinite target. *Comput. Struct*., 2003, **81**, 9-14. doi: 10.1016/S0045-7949(02)00391-7.
29. Yankelevsky, D.Z. The optimal shape of an earth penetrating projectile. *Int. J. Solids Struct*., 1983, **19**, 25-31. doi: 10.1016/0020-7683(83)90035-5.
30. LS-DYNA. Keyword user's manual. Livermore Software Technology Corporation, Livermore, California, USA; 2012, 52-54.

ACKNOWLEDGEMENT

This work was supported by the National Natural Science Foundation of China (Grant Nos.**11390363, 11532012**).

CONTRIBUTORS

Mr Jun Wu is pursuing his PhD at Beijing Institute of Technology. His research areas are impact engineering and finite element simulation.
His contribution to the current study includes approach, test verification, simulation work and paper writing.

Dr Jianguo Ning, currently working as a Professor at State Key Laboratory of Explosion Science and Technology, Beijing Institute of Technology. His research interests are in explosive mechanics, computational mechanics and its application. He has published more than 100 research paper in journals.
His contribution to this study is overall guidance during the work.

Dr Tianbao Ma, currently working as an Associate Professor at State Key Laboratory of Explosion Science and Technology, Beijing Institute of Technology. His research areas include: explosive mechanics and computational mechanics.
His contribution to this study is the design and analysis of the numerical simulation.